

**How to Cite:**

Ismail, M. H., & Tawfeeq, N. A. (2022). Synthesis and characterization of Fe<sup>2+</sup>, Cu<sup>2+</sup> and Ni<sup>2+</sup> complexes with thiosemicarbazide-di-ortho-bromobenzylacetone Schiff base and evaluation of their cytotoxicity against breast cancer cells. *International Journal of Health Sciences*, 6(S7), 3716–3733. <https://doi.org/10.53730/ijhs.v6nS7.12665>

# Synthesis and characterization of Fe<sup>2+</sup>, Cu<sup>2+</sup> and Ni<sup>2+</sup> complexes with thiosemicarbazide-di-ortho-bromobenzylacetone Schiff base and evaluation of their cytotoxicity against breast cancer cells

**Maha Haqqi Ismail**

College of Science \ Anbar University \ Ramadi \ Anbar \ Iraq

**Nabeel Arif Tawfeeq**

University of Anbar \ College of Education for Women \ Department of Chemistry \ Ramadi \ Anbar \ Iraq.

**Abstract**--In this study, Schiff base is synthesized through the reactance of di-o-bromobenzylacetone with thiosemicarbazide by acid-catalyzed condensation reaction (Aldol condensation). And using the novel Schiff base to prepare three metal complexes by reacting divalent transition metals (nickel, copper, iron) with the synthesized Schiff base. The prepared compounds were characterized by mass spectrometer, infrared spectrophotometer (FTIR), visible-ultraviolet rays (UV-Vis) and both <sup>1</sup>H and <sup>13</sup>C nuclear magnetic resonance spectrometer (NMR). The molar conductivity and magnetic susceptibility of the synthesized metal complexes were also measured. The cytotoxicity of the synthesized metal complexes against human breast cancer cell line MDA-MB231 was also measured in-vitro. All of the metal complexes were non-electrolyte and the predicted shape of these metal complexes is tetrahedral geometry. Results obtained from in-vitro cytotoxicity against breast cancer cell line type MDA-MB231 type showed that copper complex had best cytotoxicity with IC<sub>50</sub> equal to 18.5μM .

**Keywords**--Divalent metal; Schiff bases; Chalcone; Cytotoxicity; Breast cancer.

## Introduction

Transitional elements, which feature different coordination numbers, several oxidation states, and varying structural and geometric diversity of the substituted ligands, have been used by many researchers in the field

of pharmaceutical chemistry to develop anti-cancer medications (van Rijt and Sadler, 2009). The ligands have an important role in the diagnosis and treatment of diseases. When it effectively binds to the metal ion, it offers particular features to improve targeting (Chiang *et al.*, 2012). By complicating the transition elements with Schiff bases derived from thiosemicarbazide, which enhanced their biological activity, metal complexes with physiologically active and active sites offered new techniques of targeting (Perrin and Chang, 2016). Complexes have played an important role in drug innovation due to their ability to diffuse through the semi-permeable cell membrane (Prajapati and Patel, 2019). It has the capacity to function as an effective chelating agent for numerous transitional elements since it has two different types of donor atoms, nitrogen and sulfur (Mohamed, Omar and Ibrahim, 2009).

As the biological activity and flexibility of sulfur and nitrogen are related to the presence of both thioamine and amine in their composition (Stringer *et al.*, 2011). Since there have been several studies on the theoretical determination of biological activity by employing multiple programs in electronic computers to explain quantum chemistry, it was possible to clarify the biological chemical activity by experimental and computational methods (Sankaraperumal *et al.*, 2013). These estimates and predictions of biological activity are based on measuring the highest levels of occupied electron energy (HOMO) and the lowest levels of unoccupied energy (LUMO), and the energy gap between (LUMO) and (HOMO), which depends on molecules or atoms if they are soft or hard and electro-negative. The fact that biological activities depend on the separation of (HOMO) and (LUMO) in the molecule is interesting in this field. It was found that the flexural susceptibility of the inhibitor increases with increasing (HOMO) and decreasing (LUMO) in the complex ions. This is caused by electrons' capacity to move from the orbital with low energy to the orbital with high energy through electron excitation, where it can transfer to the acceptor molecules and provide electrons to other molecule (Zhang *et al.*, 2005). Additionally, the soft complexes in which the donor sulfur atoms have a small energy gap between their molecular orbitals, which easily interferes with biological molecules. As a result, the complexes' flexibility decreases as biological activity rises (Ali *et al.*, 2011). These studies are in an acidic environment that helps cancer cells grow through this point when preparing basic or neutral complexes that may work to prevent cancer (Ali, Livingstone and Phillips, 1972).

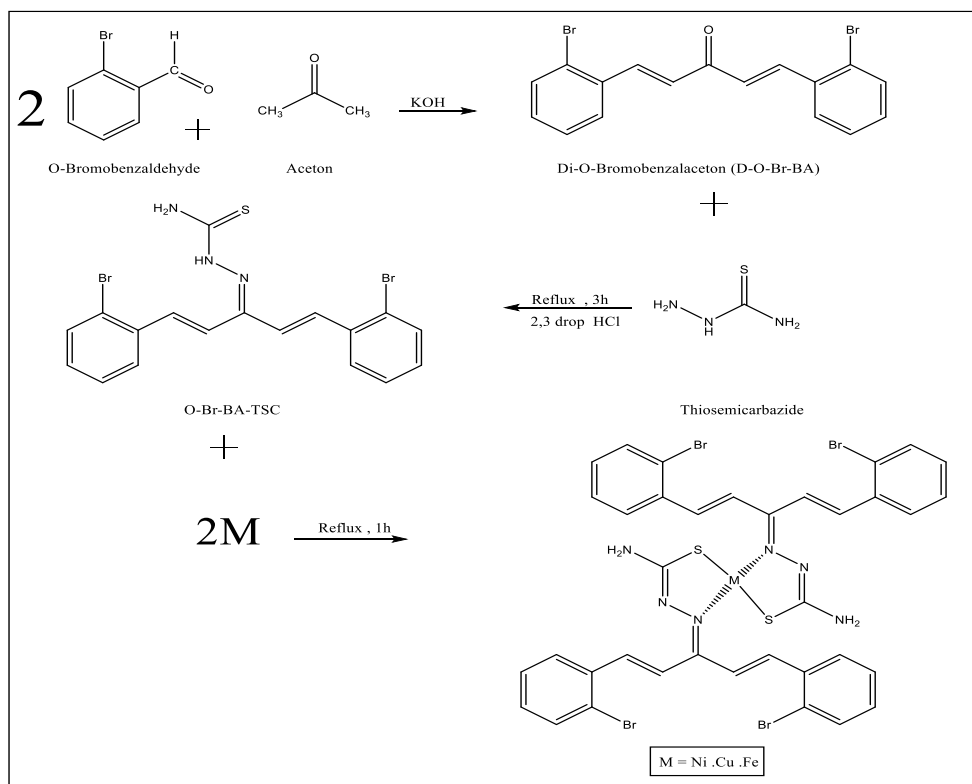


**Figure (1) Steps to prepare divalent metal complexes**

## 2 Materials and Methods

### Procedure

Chemicals: All chemicals used in the study were supplied by BDH, Sigma, and Fluka and were used as is without purification.

### synthesis of (D-o-Br-BA)1,5-Bis(2-bromo-phenyl)-penta-1,4-dien-3-one

In a Erlenmeyer flask 2.325 g of acetone was mixed with 14.9 g of orthobromobenzaldehyde dissolved in 100 mL of ethanol while stirring with a glass stirrer. An aqueous solution of potassium hydroxide, consisting of dissolving 4 grams of potassium hydroxide in 20 milliliters of distilled water, was gradually added to the mixture with stirring for half an hour. A yellow precipitate was formed, then 50 ml of cold distilled water was added to the mixture, stirring for a quarter of an hour. The mixture was filtered and recrystallized with ethanol was carried out and left to dry to obtain a pure precipitate. The yield is yellow: (14.5) grams, : m. p (103-105) °C (Vanchinathan *et al.*, 2011)(Arif Tawfeeq *et al.*, 2019).

### Synthesis of 1,5-Bis(2-bromo-phenyl)-penta-1,4-dien-3-one-Thiosemicarbazide

#### Schiff Base(D-o-Br-BA-TSC)

In a preparation flask, 7.84 g of diorthobromobenzalacetone dissolved in 50 ml of ethanol and 1.82 g of thiosemicarbazide dissolved in 25 ml of ethanol were also placed in a flask. (10-15) drops of hydrochloric acid were added gradually as a catalyst for the reaction during the reflux of the mixture for a period of 3 hours. The solution was cooled, filtered and left to dry. Re-crystallization was carried out using ethanol to obtain a pure precipitate. Color (yellow), weight (9.2 g), and melting point (157-160) °C (Islam *et al.*, 2016) (Tawfeeq *et al.*, 2019) (Alshaheri *et al.*, 2017).

### Synthesis of the complexes: (nickel - copper - zinc)

The complex formed by the reaction of binary metal chlorides with a Schiff base consisting of orthobromodibenzyl acetone with thiosemicarbazide (M-L): In a round bottom flask, dissolve 1.5 g of Schiff base in 100 ml of ethanol with stirring and heating. Heat in a second baker 0.45 g of the metal salt dissolved in 50 mL of ethanol. The metal salt was gradually added to the Schiff base. Leave the mixture to reflux for one hour to obtain a precipitate. Then the yielded precipitate was filtered and dried to give a solid precipitate. Table (1) shows the amount of prepared complexes, their percentages, colors and melting points (Dhahagani *et al.*, 2014).

**Table 1**  
**Amount of prepared complexes, percentage, color and melting point**

No	Schiff Base	Metal Complex	Weight of Complex(g)	Yield%	Color	m.p. °C
1	D-o-Br-BA-TSC	Ni-D-o-Br-BA-TSC	1.9	59 %	Yellowish green	294 d
2		Cu-D-o -Br-BA-TSC	1.76	55 %	Dark brown	181-183
3		Fe-D-o-Br-BA-TSC	1.7	53 %	Red	201 d

### Analytical and physical measurements

Melting or dissociation degrees of Chalcone, Schiff base and complexes were measured in the Department of Chemistry/ College of Education for Women/ University of Anbar using a device Model: DMP-500, Artist of science. Also, the electrical conductivity of the prepared complexes was measured using a device, Starte Ohaus, using ethanol solvent concentration ( 3-10) molar and at a temperature of 25°C. The magnetic sensitivity of solid complexes was measured at laboratory temperature (25°C) using a Balance Magnetic Susceptibility Model-M.S.B Auto device (United Kingdom), in the Department of Chemistry - College of Science - Al-Mustansiriya University. By applying the following relationship for this device, then obtaining the gram-magnetic sensitivity of Xg for the complex, as shown below:

$$X_g = (L/M) \times C \times 10^{-9} (R - R_0) \theta$$

where C calibration = 1, L = device tube length, R<sub>0</sub> = device read empty tube, R = measurement for the sample and tube, m = sample weight.

The infrared spectra for the chalcone, the base Schiff (ligand), and its complexes were acquired at the College of Education for Women/University of Anbar using a Shimadzu equipment and dry potassium bromide within a range (400-4000  $\text{cm}^{-1}$ ). At room temperature, a JASCO-V-650 instrument was used to record the electronic spectra of the chalcone, Schiff base, and UV-visible complexes at the Department of Chemistry/College of Education for Women/University of Anbar. At 25 oC and using an ethanol solvent, the compounds were dissolved in ethanol at a concentration of 3–10M.

At the University of Tehran in Iran, Bruker used a frequency of 400.77,100.28 MHz to record the  $^1\text{H}$ & $^{13}\text{C}$  NMR spectra of ketone, Schiff base, and nickel complex. At the University of Tehran in Iran, an Agilent (HP) Technology equipment with the criteria MS Model: 5973 Network Mass Selective Detector was used to measure the mass spectra of ketone, Schiff base, and metal complexes dissolved in chloroform.

### 3 Results and Discussions

#### Molar conductivity

To determine the structure of the ionic compounds in the solution, the complexes were dissolved in ethanol at a concentration of 10-3M and their molar conductivity was determined. All of the complexes were found to be non-ionic (Geary, 1971) as a consequence of the results , and Table (2) lists the molar conductivity values of the produced complexes.

Table 2  
values of molar conductivity of the prepared complexes

No.	Complexes	$\Lambda_M$ ( $\text{Ohm}^{-1}.\text{cm}^2.\text{mol}^{-1}$ )	Behaviour
1	Ni(L)	2	non-electrolyte
2	Cu(L)	6	non-electrolyte
3	Fe(L)	6	non-electrolyte

#### Magnetic susceptibility

Following diamagnetic correction to determine the effective magnetic moment values, the magnetic susceptibility of the produced complexes was evaluated at room temperature. It takes the shape of a tetrahedron (Cotton and G, 1989), just like the iron complex (Tsipis and Manoussakis, 1976), and Table (3) shows the magnetic susceptibility values for the produced complexes.

Table 3  
values of magnetic susceptibility of the prepared complexes.

No.	Complex	$\mu_{\text{eff}}$ (B.M)	Suggested Geometry
1	Ni (L)	Dia	Square Planar
2	Cu (L)	1.43	Tetrahedral
3	Fe (L)	4.47	Tetrahedral

### UV-Visible Spectrophotometer

By dissolving them in ethanol, the UV spectra of chalcone, Schiff bases, and complexes was determined, and the findings are shown in Table (4). where the chalcone absorption peak was at 320 nm (3125  $\text{cm}^{-1}$ ) Figure (2) due to the electron transitions  $n \rightarrow \pi^*$ . The absorption peak of the Schiff base appeared at 328 nm (30487  $\text{cm}^{-1}$ ) and 345 nm (28985  $\text{cm}^{-1}$ ) Fig. (3) and this is due to the electronic transitions  $\pi \rightarrow \pi^*$  and  $n \rightarrow \pi^*$ , The difference in the displacement of the ligand between the chalcone and the Schiff base is evidence of the occurrence of the reaction (Ronconi *et al.*, 2005). The complexes' UV measurements revealed absorption values as a result of their characteristic d-d transitions. Figure (4) from Nickel with Schiff Base illustrates a peak at 615 nm (16260  $\text{cm}^{-1}$ ) caused by the  ${}^3A_{2g} \rightarrow {}^3T_{2g}$  transitions and attributed to the square planar geometry (Ghosh, Wondimagegn and Parusel, 2000). Copper with Schiff base exhibits a peak at 615 nm (16260  $\text{cm}^{-1}$ ) in Figure (5), which is a part of the  ${}^2B_1 \rightarrow {}^2A_1$  transitions. Tetrahedral shape is thought to be responsible for this transition (Salih *et al.*, 2020). In Figure (6), the iron with (L) displayed a peak at 618 nm (16181  $\text{cm}^{-1}$ ), which is a  ${}^5E \rightarrow {}^5T_2$  transition. The tetrahedral form is thought to be responsible for this transition (Fabiya and Olanrewaju, 2019).

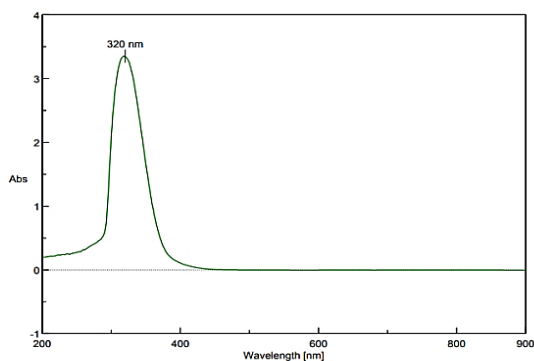


Figure (2) UV-visible spectrum of ketones

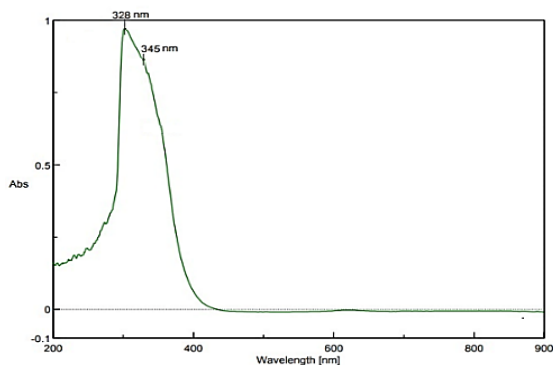


Figure (3) UV-Visible Spectrophotometer for Schiff Base

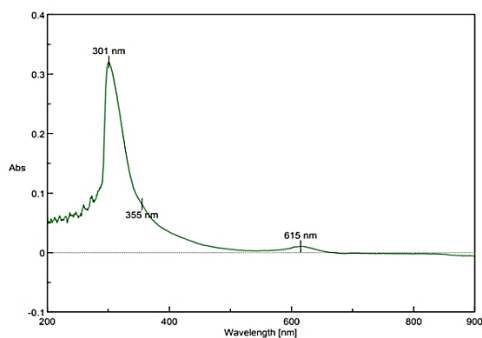


Figure (4) UV-visible spectrum of copper complex

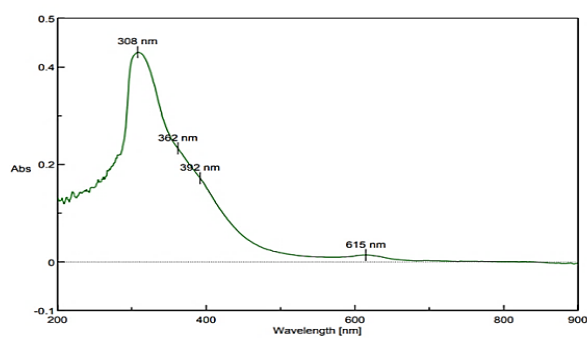


Figure (5) UV-visible spectrum of copper complex

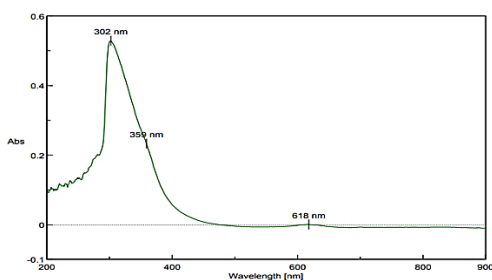


Figure (6) UV-visible spectrum of iron complex.

Table (4) UV spectrophotometric data for ketones, Schiff bases and complexes.

Comp.	Conc. mol/L	Band Position $\lambda$ nm	Wave number ( $\text{cm}^{-1}$ )	Assignment	Suggested geometry
D-o -Br- BA	$1 \times 10^{-3}$	320	3125	$\pi \rightarrow \pi^*$ $n \rightarrow \pi^*$	
D-o-Br- BA-TSC	$1 \times 10^{-3}$	328 345	30487 28985	$\pi \rightarrow \pi^*$ $n \rightarrow \pi^*$	
Ni(L)	$1 \times 10^{-3}$	301 355 615	33222 28169 16260	$\pi \rightarrow \pi^*$ $n \rightarrow \pi^*$ ${}^3A_{2g} \rightarrow {}^3T_{2g}$	Square Planar
Cu(L)	$1 \times 10^{-3}$	308 362 392 615	32467 27624 25510 16260	$\pi \rightarrow \pi^*$ $n \rightarrow \pi^*$ C.T ${}^2B_1 \rightarrow {}^2A_1$	Tetrahedral
Fe(L)	$1 \times 10^{-3}$	302 359 618	33112 27855 16181	$\pi \rightarrow \pi^*$ $n \rightarrow \pi^*$ ${}^5E \rightarrow {}^5T_2$	Tetrahedral

## Infrared spectrum

The prepared ketone was diagnosed spectrophotometrically by FT-IR spectrum, Figure (7). In it we notice the appearance of the stretching-vibration absorption bands of the double bond ( $\nu\text{C}=\text{C}$  ring & alkene) that appear within the range ( $1465\text{-}1592\text{ cm}^{-1}$ ) for compounds. A characteristic absorption band appears due to the stretching vibration of the carbonyl group ( $\nu\text{C}=\text{O}$ ) at wave number ( $1647\text{ cm}^{-1}$ ). The prepared Schiff base was also identified as in Figure (8), for the prepared ligand. It show the disappearance of the stretching vibration band for the carbonyl group ( $\nu\text{C}=\text{O}$ ) and the appearance of the stretching vibration band for azomethine group ( $\nu\text{C}=\text{N}$ ) at ( $1620\text{ cm}^{-1}$ ). The stretching vibration band of the hydrogen atoms in the aromatic ring ( $\nu\text{C-Harom}$ ) appears at ( $3055\text{ cm}^{-1}$ ). An absorption band specific to the bond ( $\nu\text{C}=\text{S}$ ) appears at ( $1164\text{ cm}^{-1}$ ). The appearance of a band-specific absorption for the bond ( $\nu\text{NH-NH}_2$ ) at ( $3422\text{-}3254\text{ cm}^{-1}$ ). The appearance of these absorption bands is a preliminary evidence for the correctness of the procedure used in preparing the ligand (Ravoof *et al.*, 2010). Table (5) shows the absorption values of ketones and the prepared Schiff base. Figures (9–11) of the prepared complexes show that the stretch-absorbing vibration bands of the azomethine group ( $\nu\text{C}=\text{N}$ ) appeared at the range ( $1637\text{-}1603$ )  $\text{cm}^{-1}$ . In addition, the ( $\nu\text{C-Harom}$ ) stretch-absorbing vibration bands appeared at the range ( $3057\text{-}3021\text{ cm}^{-1}$ ) and the (M-N  $\nu$ ) band appeared at the  $596\text{-}500\text{ cm}^{-1}$  range. The appearance of these packages is taken into consideration as a preliminary indicator of the efficacy of the procedure for these complexes (Sankaraperumal *et al.*, 2013). Table (6) shows the absorption values of the complexes prepared in this research.

Table 5  
Infrared absorption bands values for the prepared ketone and Schiff base measured in  $\text{cm}^{-1}$ .

Comp.	$\nu\text{C-H}$ Arom.	$\nu\text{C}=\text{O}$ Ketone.	$\nu\text{C}=\text{C}$ ring		$\nu\text{C}=\text{S}$	Others
D-o-Br-BA	3061	1647	1592	1465		C-Br at 755
D-o-Br-BA-TSC	3055	1620	1599	1466	1164	NH <sub>2</sub> and NH 3422,3254 C-Br at 752

Table 6  
Infrared absorption bands values for the prepared complexes measured in  $\text{cm}^{-1}$

Comp. Symb.	$\nu\text{C-H}$ Arom.	$\nu\text{C}=\text{N}$	$\nu\text{C}=\text{C}$ ring		Others	M-N	M-S
Ni(L)	3056	1637	160 7	143 9	NH <sub>2</sub> , 3349, 3256 C-Br 703	596	480
Cu(L)	3021	1604	155 9	144 0	NH <sub>2</sub> 3435, 3320 C-Br 752	527	459
Fe (L)	3057	1603	157 0	146 6	NH <sub>2</sub> 3435, 3320 C-Br 752	500	465



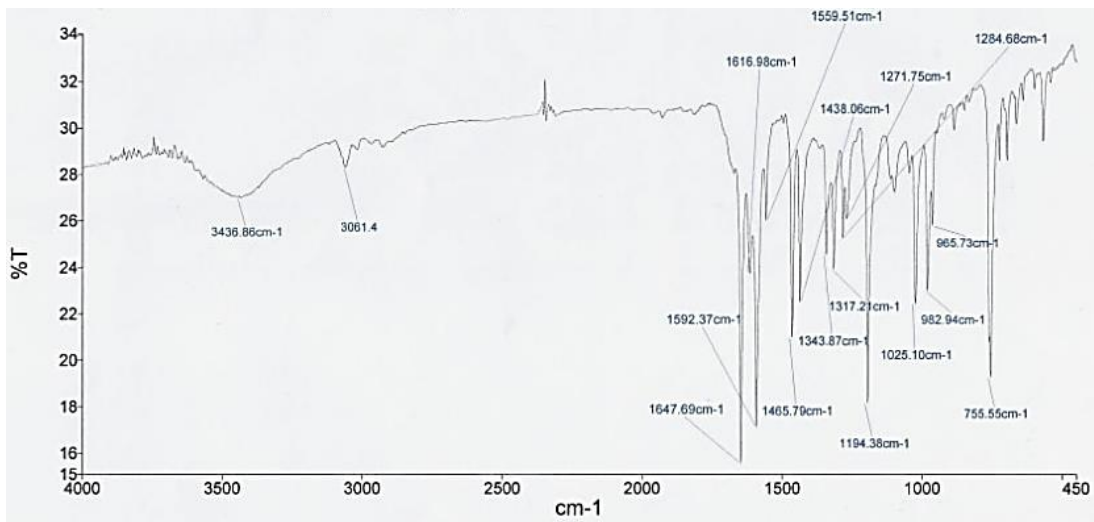


Figure (7) Infrared spectrum of the compound D-o-Br-BA.

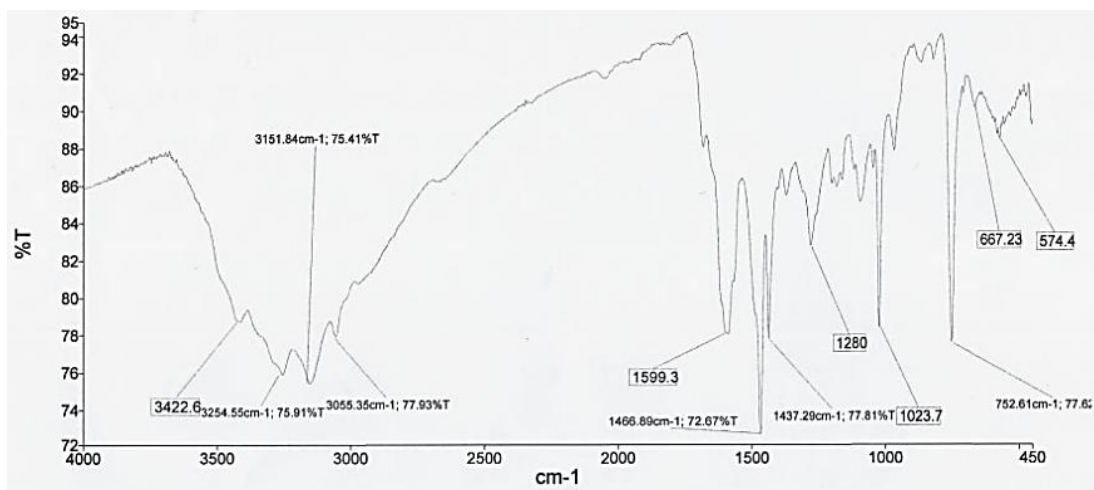


Figure (8) Infrared spectrum of the compound D-o-Br-BA-TSC.

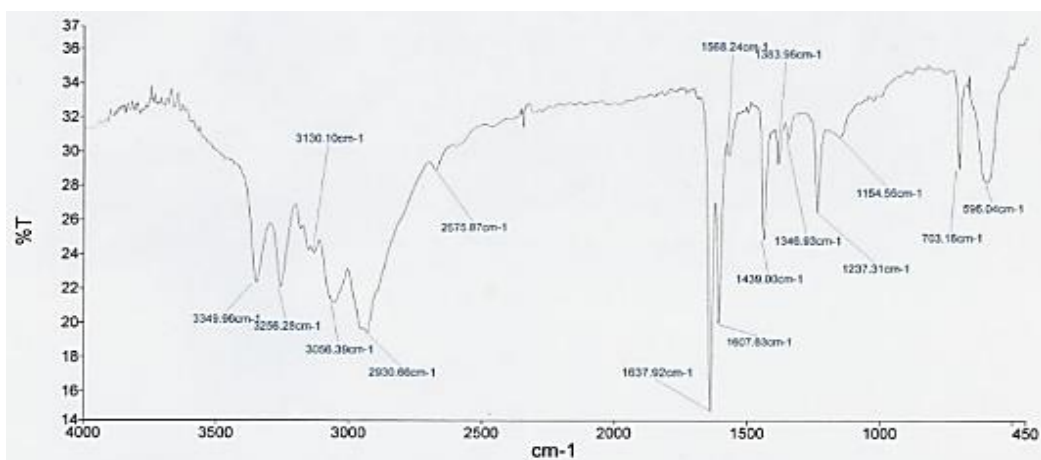


Figure (9) Infrared spectrum of the nickel complex Ni(L).

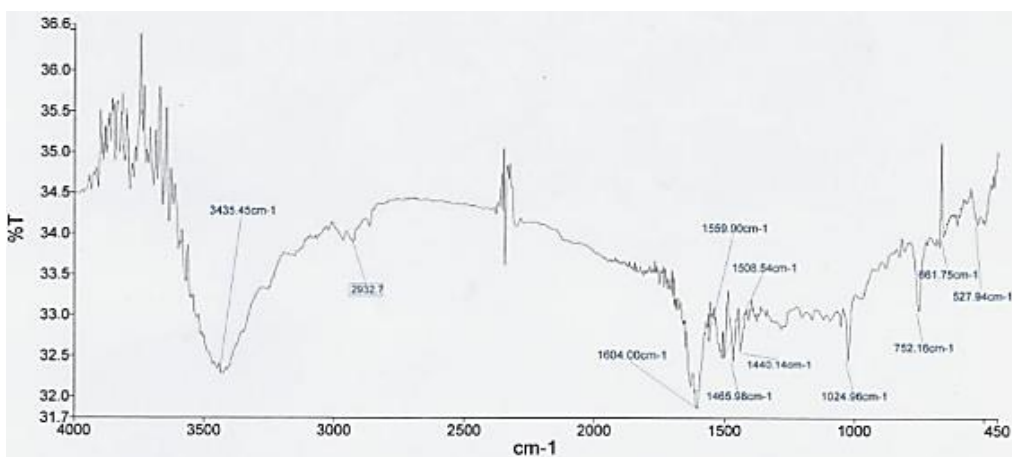


Figure (10) Infrared spectrum of Cu(L) complex.

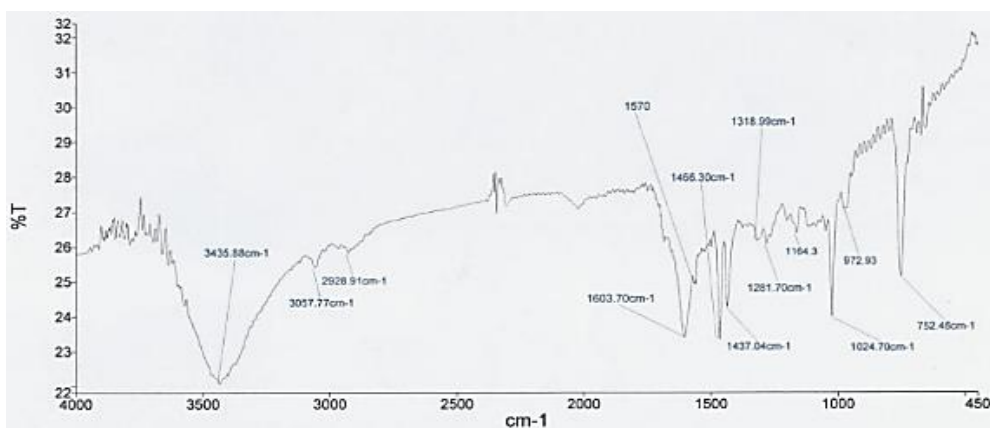


Figure (11) Infrared spectrum of Fe(L) iron complex.

### The nuclear magnetic resonance spectrum of the proton and carbon

The prepared compound (D-O-Br-BA) showed a doublet peak at  $[\delta=(8.25-8.29)$  ppm,(d,2H), =CH] belonging to the alkene group, where the integral area of this peak indicated the validity of its return, which is equal to two protons. Multiple peaks appeared at  $[\delta=(7.34-7.84)$ ppm,(m,8H),-Ar-H.] belonging to the aromatic ring protons and with an integral area of eight protons, and a doublet peaks appeared at  $[\delta=(6.61-6.64)$ ppm, (d,2H) , =CH] belongs to the alkene group, as the integral area of this sign indicates the validity of its return, which is equal to two protons (Gottlieb, Kotlyar and Nudelman, 1997) Figure (12). The prepared Schiff base (L) showed a singlet peak at  $[\delta=(11.43)$  ppm, (s,1H), -NH-N] belonging to the amine group, and the integral area of this peak indicated that its return is correct, which is equal to one proton. The singlet peak appeared at  $[\delta = (7.88)$  ppm, (s, 2H), -NH<sub>2</sub>.] due to the protons of the amine-terminal group and with an integrative area of two protons, and a multiple signal appeared at  $[\delta = (7.31-7.68)$  ppm, (m, 8H).] ), -Ar-H.] belongs to the aromatic ring protons and has an integral area of eight protons. Doublet peaks appeared at  $[\delta=(7.06-7.09)$ ppm,(d,2H),=CH] belonging to the alkene group, and the integral area of these peaks indicated the validity of its return, which is equal to two protons, doublet peaks showed at  $[\delta=(5.66-5.70)]$  ppm ,(d,2H) , =CH] belongs to the alkene group, as the integral area of this sign indicates the validity of its return, which is equal to two protons (Hazra *et al.*, 2009). Figure (13) and Table 7 show the chemical displacement of the prepared compounds by <sup>1</sup>H-NMR spectrum.

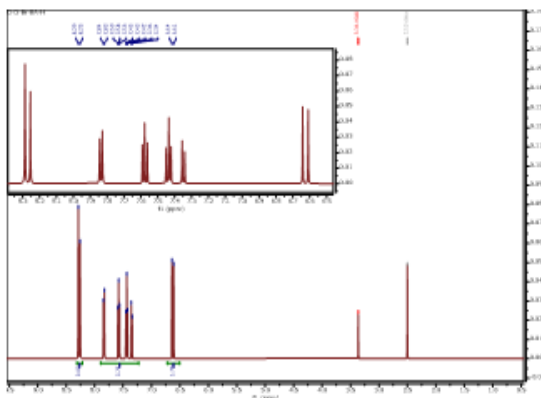


Figure (12) Expanded and condensed <sup>1</sup>H-NMR spectrum of the compound D-o-Br-BA.

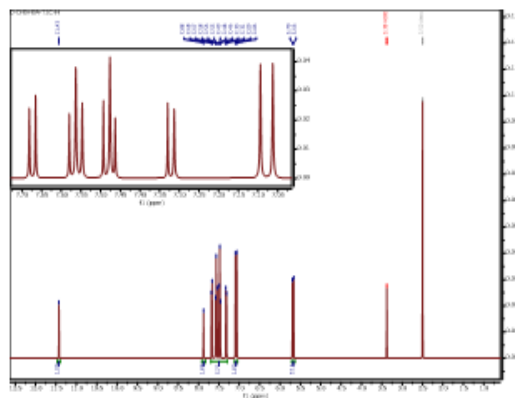


Fig. 13 Expanded and condensed <sup>1</sup>H-NMR spectrum of the compound D-o-Br-BA-TSC.

Table (7) The chemical displacement of ketones diagnosed by <sup>1</sup>H-NMR spectrum measured in ppm.

Comp. Symb.	Chemical Shift(ppm)	No. of Protons	Type of signal	Group
D-o-Br-BA	6.61-6.64	2	d	CH=CH
	7.34-7.84	8	m	Aro. Protons
	8.25-8.29	2	d	CH=CH
D-o-Br-BA-TSC	5.66-5.70	2	d	CH=CH
	7.06-7.09	2	d	CH=CH

7.31-7.68	10	m	Ar. Protons
7.88	2	s	-NH <sub>2</sub>
11.43	1	s	-NH-

## Mass Spectrum

By separating the components of the sample based on their mass and molecular weight, mass spectra can be used to determine the molecular formula of the compounds since it displays successive fragments related to the main compound.

1. Mass spectrum of ketones: The mass spectrum of the compound D-o-Br-BA showed a peak at 392.0 m/z, which represents the molecular weight of the compound (M<sup>+</sup>) (C<sub>17</sub>H<sub>12</sub>Br<sub>2</sub>O) as shown in Figure (14) below.
2. Schiff base mass spectrum: The mass spectrum of D-O-Br-BA-TSC showed a peak at 464.9 m/z which represents the molecular weight of the compound (M<sup>+</sup>) (C<sub>18</sub>H<sub>15</sub>Br<sub>2</sub>N<sub>3</sub>S) as shown in Figure (15) below.

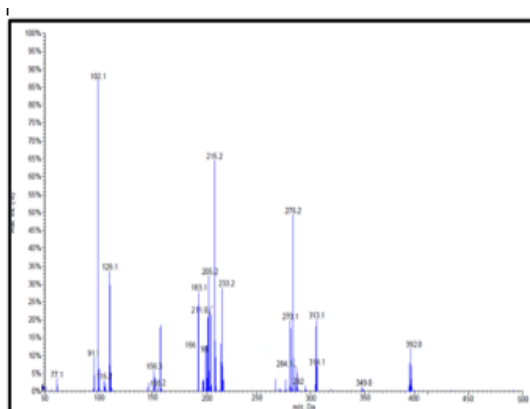


Figure (14) Mass spectrum of the compound D-o-Br-BA

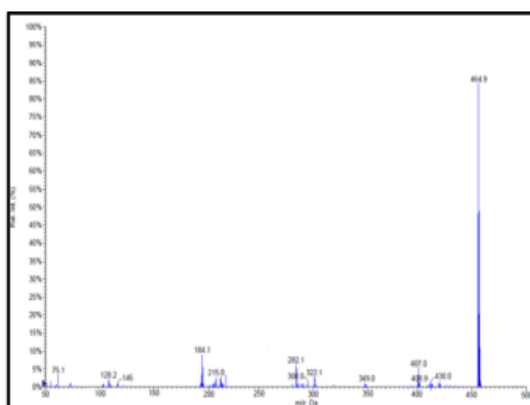


Figure (15) mass spectrum of Schiff base D-o-Br-BA-TSC

- 3- Mass spectrum of the complexes: The mass spectrum of the nickel complex Ni(L) showed a peak at 1007.2 m/z, which represents the molecular weight of the compound (M<sup>+</sup>) (C<sub>36</sub>H<sub>30</sub>Br<sub>4</sub>N<sub>6</sub>NiS<sub>2</sub>) as shown in Figure (16) below.

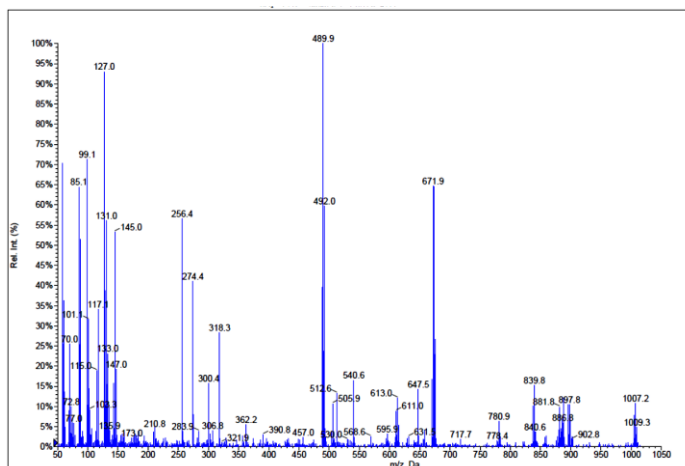


Figure (16) mass spectrum of nickel complex.

The mass spectrum of the Cu(L<sub>2</sub>) complex showed a peak at 991.9 m/z, which represents the molecular weight of the compound (M<sup>+</sup>) (C<sub>36</sub>H<sub>28</sub>Br<sub>4</sub>CuN<sub>6</sub>S<sub>2</sub>) as shown in Figure (17). The mass spectrum of the iron complex Fe(L<sub>2</sub>) showed a peak at 984.3 m/z, which represents the molecular weight of the compound (M<sup>+</sup>) (C<sub>36</sub>H<sub>28</sub>Br<sub>4</sub>FeN<sub>6</sub>S<sub>2</sub>) as shown in Figure (18) below.

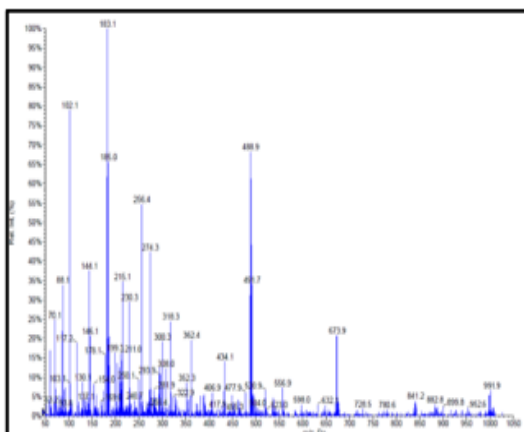


Figure (17) mass spectrum of copper complex.

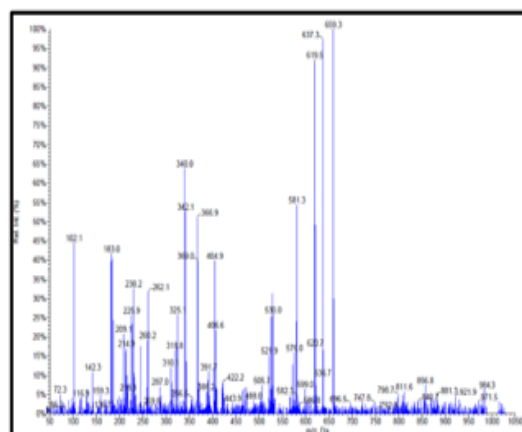


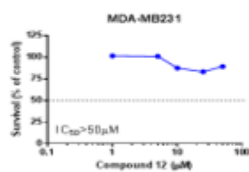
Figure (18) mass spectrum of iron complex.

### Biological activity against breast cancer

The group of cells known as cancer cells are those that escape from the normal growth in different cells in the human body and then work to change the remaining healthy cells in the affected tissue or organ. One of the many cancerous diseases that a considerable measure impact women while having a smaller impact on men is breast cancer. The ability of cancer cells to resist treatment or medication, as it seek to find a new resistance or mechanism to resist and overcome the drug, is one of the most significant obstacles facing the process of treating diseases or cancer cells. Therefore, in order to overcome the

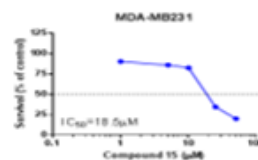
drug resistance property of cancer cells, the medicine utilized or made must have two crucial characteristics: first, it must have an anti-resistance property, and second, it must be multifunctional. When a medication binds to cancer cells' DNA, this bond causes the DNA curve to become irregular, which prevents the production of RNA (Pasikanti *et al.*, 2010).

Using the findings above as a basis, this study intends to develop a drug or treatment that is effective against cancer cells in general and against breast cancer cells in particular. In this study, the MTT method—a well-known technique—was used to examine the produced metal complexes' efficiency against breast cancer cells for the first time. Breast cancer cells are known to come in a variety of forms. The MDA-MB231 breast cancer cell type was the focus of this investigation, which also examined the impact of newly synthesized metal complexes. For each of the nine complexes, the IC<sub>50</sub> was calculated using specific concentrations of the complexes dissolved in dimethylsulfoxide (DMSO), a good complex-solvent and a negative standard. Breast cancer cells are known to come in a variety of forms. The MDA-MB231 breast cancer cell type was the focus of this investigation, which also examined the impact of newly synthesized metal complexes. For each of the nine complexes, the IC<sub>50</sub> was calculated using specific concentrations of the complexes dissolved in dimethylsulfoxide (DMSO), a good complex-solvent and a negative standard. Figures (19) to (21) represent the graph and the results obtained from measuring the biological activity of the compounds prepared in this study on MDA-MB231 breast cancer cells in vitro by culture of cancer cells ex vivo using the well-known MTT method in sources (Tawfeeq and Mohamed Ibrahim Mohamed Tahir, 2019)(Mosmann, 1983). Table (8) shows the efficacy of the metal complexes prepared in this study against MDA-MB231 breast cancer cells, and the IC<sub>50</sub> values for each of the complexes.



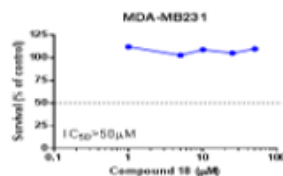
	CV	1µM	5µM	10µM	25µM	50µM
Compound 12	0.280	0.286	0.280	0.232	0.237	0.281
		0.241	0.251	0.232	0.213	0.252
		0.327	0.319	0.271	0.250	0.217
AVERAGE	0.28	0.285	0.2833333	0.245	0.233	0.25
% Survival	100	101.7	101.19048	87.5	83.33	89.29

Figure (19) Results obtained for measuring the IC<sub>50</sub> of the nickel complex



	CV	1µM	5µM	10µM	25µM	50µM
Compound 15	0.370	0.368	0.325	0.295	0.318	0.075
		0.279	0.320	0.318	0.125	0.073
		0.357	0.310	0.304	0.139	0.073
AVERAGE	0.37	0.335	0.318	0.306	0.127	0.074
% Survival	100	90.48	86.07	82.65	34.43	19.92

Figure (20) Results obtained for measuring the IC<sub>50</sub> of copper complex



	CV	1µM	5µM	10µM	25µM	50µM
Compound 18	0.292	0.346	0.326	0.300	0.312	
		0.316	0.311	0.328	0.319	0.328
		0.339	0.245	0.301	0.304	0.322
AVERAGE	0.292	0.328	0.301	0.318	0.308	0.321
% Survival	100	112.2	103	109.1	105.4	109.9

Figure (21) The results obtained for measuring the IC<sub>50</sub> of iron complex.

Table (8)  
Efficacy of metal complexes against MDA-MB231 breast cancer cells.

NO.	Complexes	IC <sub>50</sub>
1	Ni-o-Br-DBC-TSC	>50 $\mu$ M
2	Cu-o-Br-DBC-TSC	18.5 $\mu$ M
3	Fe-o-Br-DBC-TSC	>50 $\mu$ M

## Conclusion

Because copper has the ability to penetrate the lipid membrane of the cancer cell and because the ligand used, thiosemicarbazide, helped to transport the compound and direct it to the specific site of the cancer cell, these results demonstrated that the copper complex had a very strong activity against cancer cells, particularly breast cancer MDA-MB231 type.

## References


- Ali, M. A. *et al.* (2011) 'Preparation and structural characterization of nickel(II), cobalt(II), zinc(II) and tin(IV) complexes of the isatin Schiff bases of S-methyl and S-benzylthiocarbazates', *Polyhedron*, 30(4), pp. 556–564. doi: 10.1016/J.POLY.2010.11.016.
- Ali, M. A., Livingstone, S. E. and Phillips, D. J. (1972) 'Metal chelates of dithiocarbamic acid and its derivatives. III. Complexes of the tridentate schiff base  $\alpha$ -N-Methyl-S-methyl- $\beta$ -N-(2-pyridyl)methylendithiocarbamate with some 3d metal ions', *Inorganica Chimica Acta*, 6(C), pp. 11–16. doi: 10.1016/S0020-1693(00)91750-X.
- Alshaheri, A. A. *et al.* (2017) 'Synthesis, characterisation and catalytic activity of dithiocarbamate Schiff base complexes in oxidation of cyclohexane', *Journal of Molecular Liquids*, 240, pp. 486–496. doi: 10.1016/J.MOLLIQ.2017.05.081.
- Arif Tawfeeq, N. *et al.* (2019) 'Crystal structure and Hirshfeld surface analysis of a conformationally unsymmetrical bischalcone: (1 E,4 E)-1,5-bis(4-bromophenyl)penta-1,4-dien-3-one', *Acta Crystallographica Section E: Crystallographic Communications*, 75, pp. 774–779. doi: 10.1107/S2056989019006480.
- Chiang, L. *et al.* (2012) 'Multifunctional ligands in medicinal inorganic chemistry--current trends and future directions', *Current topics in medicinal chemistry*, 12(3), pp. 122–144. doi: 10.2174/156802612799078973.
- Cotton, F. A. and G. W. (1989) 'Advanced Inorganic Chemistry, Fifth Edition', *Journal of Chemical Education*, 66(3), pp. 485–486. Available at: <http://dx.doi.org/10.1021/ed066pA104.2> (Accessed: 25 July 2022).
- Dhahagani, K. *et al.* (2014) 'Synthesis and spectral characterization of Schiff base complexes of Cu(II), Co(II), Zn(II) and VO(IV) containing 4-(4-aminophenyl)morpholine derivatives: antimicrobial evaluation and anticancer studies', *Spectrochimica acta. Part A, Molecular and biomolecular spectroscopy*, 117, pp. 87–94. doi: 10.1016/J.SAA.2013.07.101.
- Fabiyi, F. S. and Olanrewaju, A. A. (2019) 'Synthesis, Characterization, Thermogravimetric and Antioxidant Studies of New Cu(II), Fe(II), Mn(II), Cu(II), Zn(II), Co(II) and Ni(II) Complexes with Benzoic Acid and 4,4,4-Trifluoro-1-(2-naphthyl)-1,3-butanedione', *International Journal of Chemistry*,


- 11(1), p. p60. doi: 10.5539/IJC.V11N1P60.
- Geary, W. J. (1971) 'The use of conductivity measurements in organic solvents for the characterisation of coordination compounds', *Coordination Chemistry Reviews*, 7(1), pp. 81–122. doi: 10.1016/S0010-8545(00)80009-0.
- Ghosh, A., Wondimagegn, T. and Parusel, A. B. J. (2000) 'Electronic Structure of Gallium, Copper, and Nickel Complexes of Corrole. High-Valent Transition Metal Centers versus Noninnocent Ligands', *Journal of the American Chemical Society*, 122(21), pp. 5100–5104. doi: 10.1021/JA9943243.
- Gottlieb, H. E., Kotlyar, V. and Nudelman, A. (1997) 'NMR chemical shifts of common laboratory solvents as trace impurities', *Journal of Organic Chemistry*, 62(21), pp. 7512–7515. doi: 10.1021/JO971176V/ASSET/IMAGES/JO971176V.SOCIAL.JPEG\_V03.
- Hazra, S. *et al.* (2009) 'Syntheses, structures, absorption and emission properties of a tetraaminodiphenol macrocyclic ligand and its dinuclear Zn(II) and Pb(II) complexes', *Polyhedron*, 28(14), pp. 2871–2878. doi: 10.1016/J.POLY.2009.06.039.
- Islam, M. A. A. A. *et al.* (2016) 'Benzyl 3-(3,4,5-trimethoxybenzylidene)dithiocarbamate', *IUCrData*, 1(2). doi: 10.1107/S2414314616001905.
- Mohamed, G. G., Omar, M. M. and Ibrahim, A. A. (2009) 'Biological activity studies on metal complexes of novel tridentate Schiff base ligand. Spectroscopic and thermal characterization', *European Journal of Medicinal Chemistry*, 44(12), pp. 4801–4812. doi: 10.1016/J.EJMECH.2009.07.028.
- Mosmann, T. (1983) 'Rapid colorimetric assay for cellular growth and survival: application to proliferation and cytotoxicity assays', *Journal of immunological methods*, 65(1–2), pp. 55–63. doi: 10.1016/0022-1759(83)90303-4.
- Pasikanti, K. K. *et al.* (2010) 'Noninvasive urinary metabonomic diagnosis of human bladder cancer', *Journal of Proteome Research*, 9(6), pp. 2988–2995. doi: 10.1021/PR901173V.
- Perrin, C. L. and Chang, K. L. (2016) 'The Complete Mechanism of an Aldol Condensation', *Journal of Organic Chemistry*, 81(13), pp. 5631–5635. doi: 10.1021/ACS.JOC.6B00959/SUPPL\_FILE/JO6B00959\_SI\_001.PDF.
- Prajapati, N. P. and Patel, H. D. (2019) 'Novel thiosemicarbazone derivatives and their metal complexes: Recent development', <https://doi.org/10.1080/00397911.2019.1649432>, 49(21), pp. 2767–2804. doi: 10.1080/00397911.2019.1649432.
- Ravoof, T. B. S. A. *et al.* (2010) 'Synthesis, characterization and biological activities of 3-methylbenzyl 2-(6-methyl pyridin-2-ylmethylene)hydrazine carbodithioate and its transition metal complexes', *Transition Metal Chemistry*, 35(7), pp. 871–876. doi: 10.1007/S11243-010-9406-6.
- van Rijt, S. H. and Sadler, P. J. (2009) 'Current applications and future potential for bioinorganic chemistry in the development of anticancer drugs', *Drug discovery today*, 14(23–24), p. 1089. doi: 10.1016/J.DRUDIS.2009.09.003.
- Ronconi, L. *et al.* (2005) 'Gold dithiocarbamate derivatives as potential antineoplastic agents: design, spectroscopic properties, and in vitro antitumor activity', *Inorganic chemistry*, 44(6), pp. 1867–1881. doi: 10.1021/IC048260V.
- Salih, B. D. *et al.* (2020) 'Biological activity and laser efficacy of new Co (II), Ni (II), Cu (II), Mn (II) and Zn (II) complexes with phthalic anhydride', *Materials Today: Proceedings*, 43, pp. 869–874. doi: 10.1016/J.MATPR.2020.07.083.
- Sankaraperumal, A. *et al.* (2013) 'Nickel(II) complex of p-[N,N-bis(2-



- chloroethyl)amino]benzaldehyde-4-methyl thiosemicarbazone: Synthesis, structural characterization and biological application', *Polyhedron*, 50(1), pp. 264–269. doi: 10.1016/J.POLY.2012.11.006.
- Suryasa, I. W., Rodriguez-Gámez, M., & Koldoris, T. (2021). The COVID-19 pandemic. *International Journal of Health Sciences*, 5(2), vi-ix. <https://doi.org/10.53730/ijhs.v5n2.2937>
- Stringer, T. *et al.* (2011) 'Mono- and dinuclear ( $\eta^6$ -arene) ruthenium(II) benzaldehyde thiosemicarbazone complexes: Synthesis, characterization and cytotoxicity', *Inorganic Chemistry Communications*, 14(6), pp. 956–960. doi: 10.1016/J.INOCHE.2011.03.041.
- Tawfeeq, N. A. *et al.* (2019) 'Crystal structure of benzyl N'-[(1E,4E)-1,5-bis(4-methoxyphenyl)penta-1,4-dien-3-ylidene]hydrazine-1-carbodithioate', *Acta Crystallographica Section E: Crystallographic Communications*, 75(Pt 11), pp. 1613–1619. doi: 10.1107/S2056989019013458/WM5520ISUP3.CML.
- Tawfeeq, N. A. and Mohamed Ibrahim Mohamed Tahir, D. P. (2019) 'Synthesis of transition metal complexes containing symmetrical chalcone-derived Schiff bases and cytotoxic studies against bladder cancer cells.' *Universiti Putra Malaysia*.
- Tsipis, C. A. and Manoussakis, G. E. (1976) 'Syntheses and spectral study of new iodobis(dialkylthiocarbamate) complexes of arsenic, antimony and bismuth', *Inorganica Chimica Acta*, 18(C), pp. 35–45. doi: 10.1016/S0020-1693(00)95582-8.
- Vanchinathan, K. *et al.* (2011) 'Synthesis, crystal growth and characterization of 1,5-diphenylpenta-1,4-dien-3-one: An organic crystal', *Physica B: Condensed Matter*, 406(22), pp. 4195–4199. doi: 10.1016/J.PHYSB.2011.07.055.
- Zhang, H. *et al.* (2005) 'Synthesis, crystal structure, cytotoxic activity and DNA-binding properties of the copper (II) and zinc (II) complexes with 1-[3-(2-pyridyl)pyrazol-1-ylmethyl]naphthalene', *Journal of inorganic biochemistry*, 99(5), pp. 1119–1125. doi: 10.1016/J.JINORGBIO.2005.02.005.

### Biography of Authors

	<p>PhD: Nabeel Arif Tawfeeq  <a href="mailto:edw.nobel_ani_70@uoanbar.edu.iq">edw.nobel_ani_70@uoanbar.edu.iq</a>  <i>Lecturer in Inorganic Chemistry</i>  <i>University of Anbar \ College of Education for Women \ Department of Chemistry \ Ramadi \ Anbar \ Iraq.</i>  <i>ORCID No. \ 0000-0001-7018-9812</i></p>
	<p>Maha Haqqi Ismail  <a href="mailto:mah20s3009@uoanbar.edu.iq">mailto:mah20s3009@uoanbar.edu.iq</a>  <i>Master student at the College of Science \ Anbar University \ Ramadi \ Anbar \ Iraq.</i></p>

	
---	--